IMECE2008-67594

BIOMIMETIC MICROACTUATOR POWERED BY POLYMER SWELLING

Howon Lee
Department of Mechanical Science and Engineering
University of Illinois at Urbana-Champaign
Urbana, IL 61801, USA
hlee99@illinois.edu

Chunguang Xia
Department of Mechanical Science and Engineering
University of Illinois at Urbana-Champaign
Urbana, IL 61801, USA
cxia@illinois.edu

Nicholas Xuanlai Fang
Department of Mechanical Science and Engineering
University of Illinois at Urbana-Champaign
Urbana, IL 61801, USA
nicfang@illinois.edu

ABSTRACT

We propose novel biomimetic polymer microactuators. The actuation mechanism is inspired by nastic movement of the moving plant, *Mimosa pudica*, which folds its leaves upon external stimulus by regulating turgor pressure of cells in specific location. Photo-cured poly(ethylene glycol) diacrylate (PEGDA) microactuator is fabricated using projection micro-stereolithography (PµSL) capable of complex 3D micro fabrication. The swelling effect of PEG in water and organic solvent is exploited as an actuation mechanism of the device. Stress relaxation in the structure due to solvent absorption is controlled locally by delivering solvent through microfluidic channels embedded in the actuator, thereby generating a net movement in the device. Timescale of the motion derived from analytical swelling model suggests that actuation speed can be effectively increased by scaling down the actuator because the characteristic swelling time depends on the length as L^2, which is verified experimentally.

INTRODUCTION

Recent advancement in micro fabrication techniques has enabled us to design and fabricate a wide variety of micro-devices such as IC circuits and MEMS-based sensors[1]. However, it is still challenging to make microactuators in conventional concept because of difficulty in assembly and dominant effect of viscosity and friction in micro scale and below. Thus, there have been many studies to seek for novel design of microactuators, especially inspired by plant motion

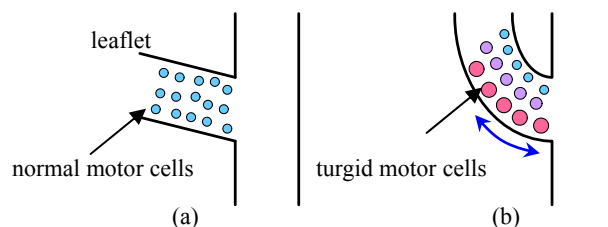*http://plantsinmotion.bio.indiana.edu/plantmotion/movements/nastic/mimosa/mimosa.html

Figure 1. *Mimosa pudica* and its moving mechanism. (a) Motor cells at pulvinus are in normal state in open leaves (b) Selective increase of turgor pressure in motor cells results in folding motion of leaves.

because moving plants move their body without any mechanical components or muscle. One of well known moving plants is *Mimosa pudica*, known also as Sensitive plant, which folds its leaves upon external disturbances such as mechanical and thermal stimulus. Once stimulated by touch or heat, *Mimosa pudica* regulates turgor pressure of motor cells located in pulvinus. Owing to the fact that swelling motor cells are

distributed mainly on one side of midrib (figure 1), each leaf undergoes bending motion in the direction where less swelling occurs[2].

Inspired by this elegant moving mechanism, we present novel microactuator powered by polymer swelling. Although many polymeric micro devices driven by swelling have been reported[3,4,5], these actuators are in simple geometry such as sphere and strip and fine control of motion and its timescale remain challenging. Furthermore, in some cases the device should be made of several different polymers or placed in solvent for actuation. In this study, we fabricated polymeric micro device using 3D parallel micro fabrication technique termed projection micro-stereolithography[6], which builds up 3D micro structure by photo-curing polymer in a layer-by-layer fashion. By virtue of complex 3D fabrication capability, we embedded microfluidic channels in the device for solvent delivery. Solvent is delivered to target locations where swelling is needed for actuation, thereby accomplishing programmable local swelling as *Mimosa pudica*.

It has been reported that timescale of plant movement is limited by characteristic poroelastic time which is proportional to the square of the smallest dimension of moving part[7]. In this work, we studied swelling mechanism of polymer based on Tanaka's theory[8] and experimentally showed that there exists a timescale of our device which is equivalent to the poroelastic time. Also, artificial micro *Mimosa pudica* with leaves was fabricated and tested for demonstration of this novel actuation mechanism.

THEORY

Tanaka and Fillmore[8] suggested that kinetics of swelling gel can be explained via stress relaxation in polymer network induced by osmotic pressure. It is assumed that polymer is under compressive stress when it is dry and that the stress is relaxed when solvent is absorbed in polymer. Polymer swelling in solvent can be represented as quasi-static force equilibrium between stress gradient in polymer and friction from solvent penetration,

$$\nabla \cdot \widetilde{\sigma} = f \frac{\partial \overline{u}}{\partial t} \tag{1}$$

where $\widetilde{\sigma}$ is the stress tensor, $\overline{u}$ is the displacement vector, and f is the friction coefficient between polymer network and solvent. Accompanied with the following constitutive equation (2), compatibility equation (3), and one dimensional assumption (4),

$$\sigma_{ik} = K\nabla \cdot \overline{u}\,\delta_{ik} + 2\mu(\varepsilon_{ik} - \frac{1}{3}\nabla \cdot \overline{u}\,\delta_{ik}) \tag{2}$$

$$\varepsilon_{ik} \equiv \frac{1}{2}\left(\frac{\partial u_k}{\partial x_i} + \frac{\partial u_i}{\partial x_k}\right) \tag{3}$$

$$\overline{u} = u(x,t) \tag{4}$$

where K, μ, and ε are bulk modulus, shear modulus, and strain, respectively, the equation (1) can be written as diffusion equation,

$$\frac{\partial u}{\partial t} = D\frac{\partial^2 u}{\partial x^2} \tag{5}$$

where $D = (K + 4\mu/3)/f$ is diffusion coefficient.

We use this equation or motion to analyze the swelling motion of cantilever beam with embedded microfluidic channel as shown in figure 2(a). From the experimental measurement of fully swollen state of polymer, we can determine the initial condition,

$$u(x,0) = \Delta L_o \frac{x}{L} \tag{6}$$

where L is initial dimension of polymer and ΔL_0 is dimensional increment at fully swollen state. Also, we assume free stress at channel-polymer interface and fixed boundary condition on the dry side as below.

$$u(0,t) = 0 \tag{7}$$

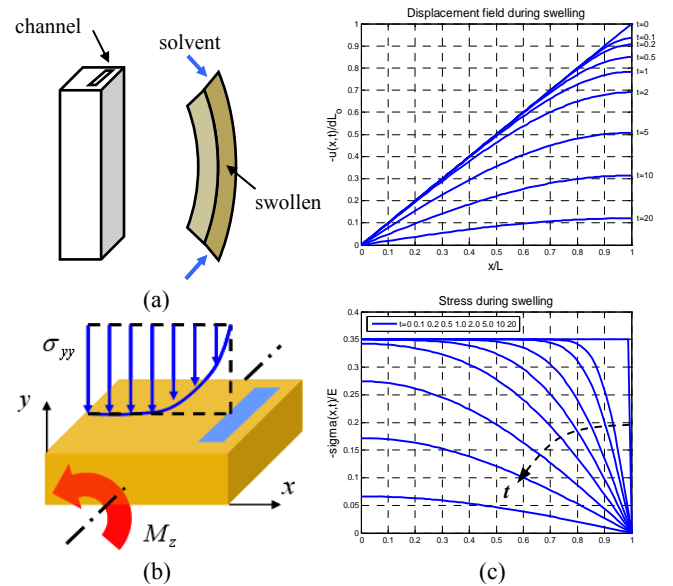$$\sigma_{xx}\big|_{x=L} = K\frac{\partial u}{\partial x}\bigg|_{x=L} = 0 \tag{8}$$

Figure 2. (a) Bending of beam caused by asymmetric swelling induced by solvent delivery through embedded channel (b) Schematic diagram of bending moment development on the cross section of beam due to non-uniform stress distribution (c) Simulated displacement field and stress relaxation along the cross section (x-dir) during swelling ($L = 75\,\mu m$, $D = 2.2 \times 10^{-10}\,m^2/s$)

By solving the equation (5) with the initial condition (6) and boundary conditions (7) and (8), we can simulate displacement field and stress relaxation in polymer during swelling. The result is shown in figure 2(c). Note that the displacement field is normalized with respect to the total increment ΔL_0 and the stress to the Young's mudulus E. To determine diffusion coefficient D, we relied on fitting to experimental result due to difficulty in measuring friction coefficient f. In addition to the numerical solution, it is well known that we can solve the diffusion equation (5) analytically using Fourier series and the characteristic time in the exact solution is $\tau = L^2/D$ [8]. Since our device is actuated by polymer swelling, this characteristic swelling time can be considered as a timescale of the actuation of our device. It has been reported that the principle of plant movement is diffusive equilibration of pressure by internal fluid transport in elastic tissue and that its timescale is characterized by poroelastic time $\tau_p \sim \mu L^2/kE$, where μ is viscosity of internal fluid and k is hydraulic permeability[7]. It is important to note that actuation mechanism of our device and moving plants bring about the similar timescale. Furthermore, the timescale depends on the dimension as L^2, which implies that we can enhance the speed of actuation effectively by reducing the size of actuator.

To simulate the motion of our device, we approximate σ_{yy} to σ_{xx} obtained above under the isotropic swelling assumption for simplicity. Then non-uniform stress distribution creates bending moment in beams as illustrated in figure 2(b) according to the following equation,

$$M_z(t) = \int_0^L \sigma_{yy}(x,t) \cdot w \cdot x \, dx \quad (9)$$

where w is the thickness of the beam in z direction. By the relationship from beam theory, angular displacement of beam can be estimated from the bending moment.

$$\theta(t) \sim \frac{M_z(t)}{I_{zz}} \quad (10)$$

Bending motion of swelling beams with different dimension in width was simulated using above equations and shown in figure 6 along with experimental result. Although we could not calculate the exact value of angle due to the lack of material properties of polymer, we see that the trend of simulated actuation and its timescale according to different dimension correspond very well with experimental result.

DESIGN AND EXPERIMENT

As a fabrication method for polymeric device with embedded microfluidic channels, we used projection micro-stereolithography(PµSL)[6] capable of complex three
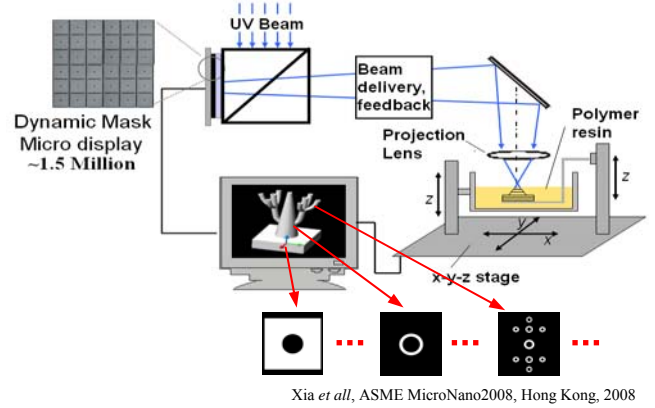
Figure 3. Projection micro stereolithography configuration. 3D CAD drawing is sliced into a set of layers and the image of each layer is sent to a dynamic mask generator. Then, a light from flood UV source is reflected off the dynamic mask and the beam containing the image is focused on the surface of polymer resin through projection lens which reduces the image to the desired size. Once a layer is polymerized, stage drops the substrate by a predefined layer thickness, and the dynamic mask displays the next image. This process proceeds iteratively until all the layers are complete.

dimensional micro fabrication in a layer-by-layer fashion with a resolution less than $2\mu m$. Figure 3 is a schematic diagram of this fabrication method. As a material, we used poly(ethylene glycol) diacrylate (PEGDA, MW575), but any photo-curable polymer that swells in solvent can be used for this device.

To understand fundamental swelling characteristics of polymer, we carried out swelling ratio test. Polymer specimen as shown in figure 4(a) was fabricated to study the effect of cross-linking ratio of polymer and actuation solvent. First pillar was polymerized under relatively lower light intensity (5.22mW/cm^2), thus has lower cross-linking density, and the second pillar was polymerized under higher light intensity (8.55mW/cm^2), thus has higher cross-linking density. Light intensity can be varied within a projection plane by using gray scale image mask shown in figure 4(b). Exposure time for each layer was 15 seconds and thickness of each layer was $25\mu m$. This specimen was transferred into ethanol, de-ionized water (DI water) and acetone in which its swelling ratio was measured through microscope (figure 4(c)) until it came into steady state. From the result shown in figure 4(d), we see that swelling ratio of lower cross-linking density is higher than that of higher cross-linking density. This is attributed to the fact that when it dries polymer with lower cross-linking density shrinks more than that with higher cross-linking density owing to its relatively loose network structure. Once placed in solvent, this shrunken polymer restores its original volume due to stress relaxation caused by solvent, which leads to the higher swelling ratio for more shrunken, or lower cross-linked polymer. In addition to cross-linking density, swelling ratio also depends on solvent. Figure 4(d) shows that swelling ratio in DI water and
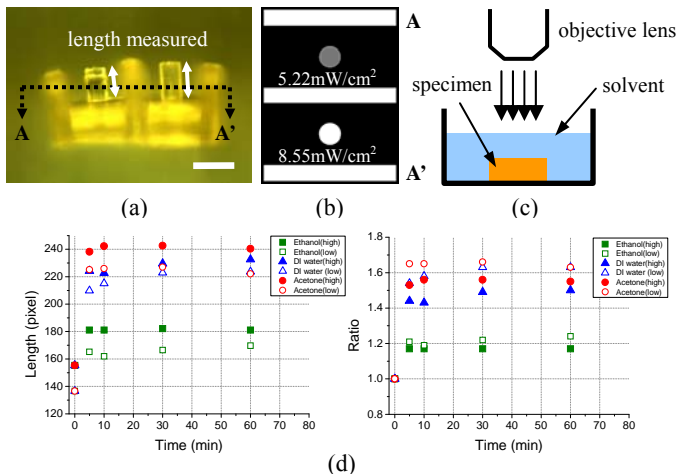
Figure 4. (a) Swelling ratio test specimen (b) Gray scale of sliced image enables light intensity control within a projection plane during fabrication (c) Experimental setup (d) Swelling ratio change during swelling. Swelling ratio is swollen length divided by the length in dry state.

acetone is comparable but larger than in ethanol. The reason for the behind this is still under investigation, but we suppose that this results from different molecular attraction between polymer and different solvent. From this result, we can conclude that swelling motion is more effective when sample with low cross-linking density is actuated by water or acetone. In this paper, we used acetone (99.8%) because of its high evaporation rate.

Taking advantage of this polymer swelling characteristics, we designed six cantilever beams with embedded microfluidic channel as shown in figure 5(a) in order to investigate the controllability of actuation timescale. All the beams are $1400 \mu m$ long and $200 \mu m$ wide. Channels are $150 \mu m \times 50 \mu m$ in cross section, and embedded $25 \mu m$ under the beam's outer surface. The dimension of the remaining part in the cross section where solvent needs to propagate to generate motion varies from $25 \mu m$ up to $275 \mu m$ with $50 \mu m$ increment, as shown in figure 5(b). When a droplet
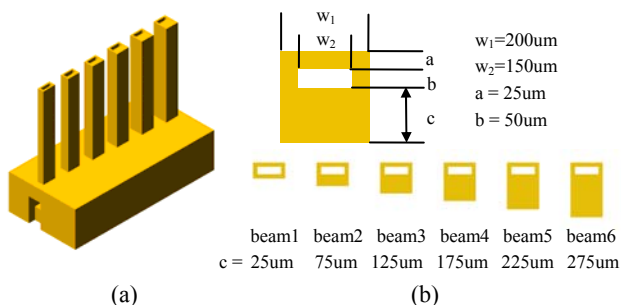

Figure 5. (a) Bending beams with embedded micro fluidic channels. (beam height: $1400 \mu m$, base: $2400 \mu m \times 1200 \mu m$) Channels are connected together in the base for simultaneous solvent delivery to all the channels (b) cross sectional dimensions of each beam
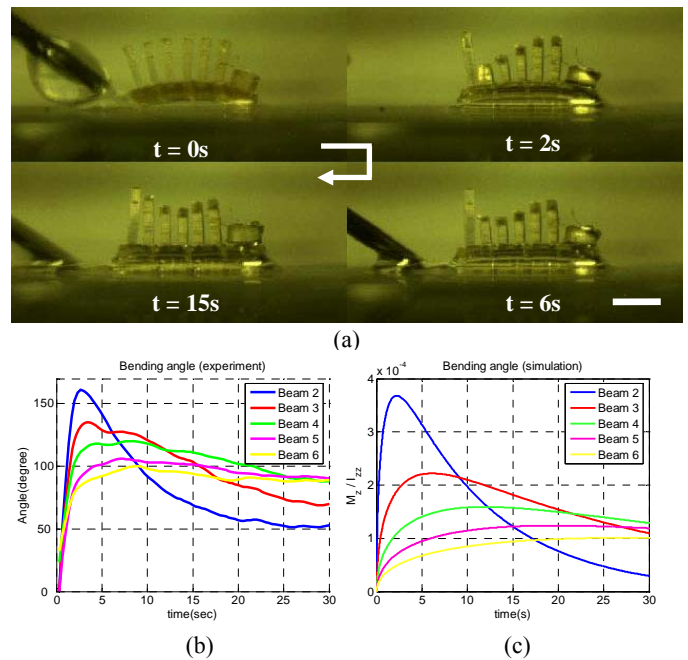

Figure 6. (a) Time-lapsed motion of bending beams during swelling actuation. Scale bar indicates $1000 \mu m$. (b) Bending angle from experiment (c) Bending angle estimated by simulation. Unit does not agree with experimental data, but the trend of actuation timescale with respect to different length scale matches very well.

of solvent is applied to the opening of the channel at the base, all the channels are filled with solvent automatically and immediately by capillary action. Then, area near the channel becomes wet first while the other side remains dry due to finite solvent penetration speed. Therefore, non-uniform stress distribution is developed because stress relaxation takes place only in wet region as explained by the theory. Consequently, different bending angle is generated in each beam depending on the dimension of cross section, resulting in different timescale of bending motion as shown in figure 6. Note that beam 1 does not bend but stretch only because of uniform stress distribution due to its symmetric cross section. Bending motion was recorded from the front of the sample as shown in figure 6(a). From this video, the distance between the tip and the base of each beam was measured and bending angle has been obtained using simple geometric relationships as shown in figure 6(b). Not only does this result verify the theoretical model presented in the previous chapter, but it also demonstrates that the actuation timescale of this device is highly tunable in design stage.

To demonstrate that the motion can be programmed by local stress control in this device, we fabricated a micro polymeric device which mimics the movement of *Mimosa pudica*. This artificial micro Mimosa consists of combination of beams as structural components and embedded capillary network for solvent delivery (figure 7(a)). Each leaflet is $1000 \mu m$ long and half of it near the base has embedded channel inside

4 Copyright ©2008 by ASME

(a)   (b)

t=0s, 82°   t=0.5s, 59°   t=2.1s, 42°

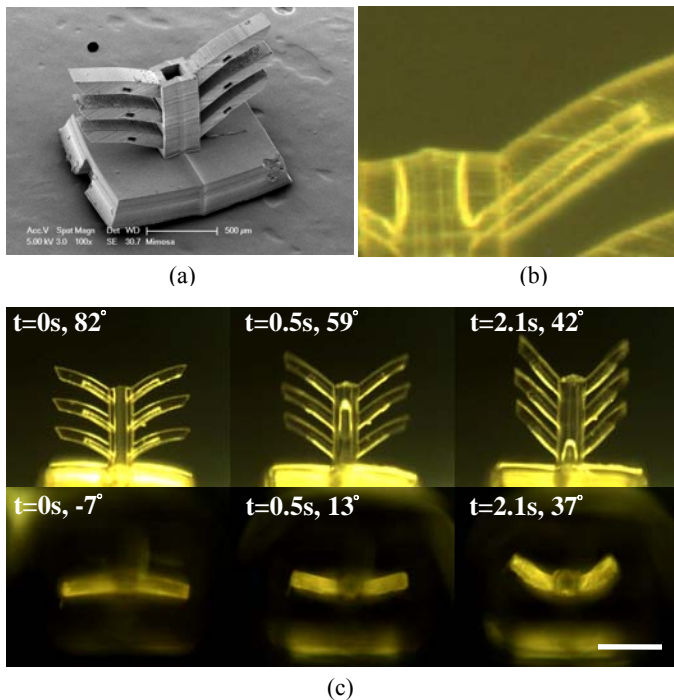t=0s, -7°   t=0.5s, 13°   t=2.1s, 37°

(c)

Figure 7. (a) Artificial micro Mimosa. (b) Embedded capillary network for solvent delivery. (c) Time-lapsed leaf folding motion of artificial micro Mimosa. Front view and top view. Scale bar indicates $500 \mu m$.

branched out from main channel (figure 7(b)). This part plays a role as a pulvinus which generates folding motion of leaves when solvent is delivered. Note that channel is located off the center axis of leaflet from both front view and top view so that bending occurs in vertical and horizontal direction simultaneously when swelling takes place. End of channels is open for an exit of the air inside as well as the ease of solvent evaporation during de-actuation (figure 7(b)). Figure 7(c) shows leaf folding motion of artificial micro Mimosa. When a solvent droplet is applied, solvent is delivered to the base of leaves immediately by capillary action, leading to a fast folding of leaves. Angle of leaves to the main post in vertical plane changes from 82° when they are open to 42° when they are completely closed at $t = 2.1s$. Also, angle in horizontal plane changes from −7° when they are open to 37° at $t = 2.1s$. In addition, this motion is completely reversible because leaves return to its open position as solvent evaporates through openings at the end of channels. This result demonstrates that stress relaxation by swelling can be controlled locally by designing capillary network accordingly, which enables fine tuning of direction of motion as well as its timescale in three dimensional space.

CONCLUSION

This paper presents a bio-inspired microactutator driven by polymer swelling. A novel fabrication technique, PµSL, offers simple and fast fabrication of sophisticated 3D micro structure. Embedded microfluidic channels in the device enables local control of stress at micro scale by delivering solvent to the specific location where swelling is needed for desired motion. Theoretical and experimental study of swelling shows that direction and speed of motion of this microactuator are highly tunable. Furthermore, this device requires no external power source but a single droplet of solvent for actuation. Also, actuation is fully reversible in that the moving components return to their original configuration as solvent evaporates. This actuation scheme has a great potential in a wide variety of applications, such as soft robotics, artificial muscle and microfluidic devices.

REFERENCES
[1] Gregory T.A. Kovacs, *Micromachined Transducers Sourcebook*, WCB/McGraw-Hill, Boston, 1998.
[2] Taya, M., Bio-inspired Design of Intelligent Materials, *EAPAD Proceedings of SPIE* Vol. 5051, 2003.
[3] Gerlach, G., Guenther, M., Sorber, J., Suchaneck, G., Arndt, K. and Richter, A., Chemical and pH sensors based on the swelling behavior for hydrogels, *Sensors and Actuators B* Vol. 111-112, 2005, 555-561.
[4] Kim, D. and Beebe, D. J., Hydrogel-based reconfigurable components for microfluidic devices, *Lab on a Chip*, 2007, 7, 193-198.
[5] Guan, J., He, H., Hansford, D. J. and Lee, J., Self-Folding of Three-Dimensional Hydrogel Microstructures, *J. Phys. Chem. B*, 2005, 109, 23134-23137.
[6] Sun, C., N. Fang, D. M. Wu, and X. Zhang. Projection Micro-Stereolithography Using Digital Micro-Mirror Dynamic Mask, *Sensors and Actuators A*, 121:1, 113-120, 2005.
[7] Skotheim, J., Mahadevan, L., Physical Limits and Design Principles for Plant and Fungal Movements, *Science*, Vol.308, 1308-1310, 2005
[8] Tanaka, T. and Fillmore, D. J., Kinetics of swelling of gels, *J. Chem. Phys.* 70(03), Feb. 1979, 1214-1218